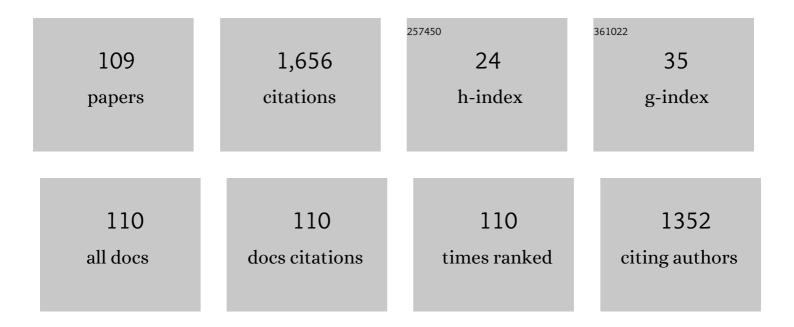


List of Publications by Year in descending order

Source: https://exaly.com/author-pdf/1974053/publications.pdf Version: 2024-02-01



#	Article	IF	CITATIONS
1	Research progress of flexible wearable pressure sensors. Sensors and Actuators A: Physical, 2021, 330, 112838.	4.1	70
2	Observation of the size-dependent blueshifted electroluminescence from nanocrystalline Si fabricated by KrF excimer laser annealing of hydrogenated amorphous silicon/amorphous-SiNx:H superlattices. Applied Physics Letters, 1998, 72, 722-724.	3.3	59
3	Full color light emission from amorphous SiCx:H with organic–inorganic structures. Journal of Applied Physics, 2000, 88, 6408-6412.	2.5	54
4	Photoluminescence characteristics from amorphous SiC thin films with various structures deposited at low temperature. Solid State Communications, 2005, 133, 565-568.	1.9	54
5	Phosphorus Doping in Si Nanocrystals/SiO2 Multilayers and Light Emission with Wavelength Compatible for Optical Telecommunication. Scientific Reports, 2016, 6, 22888.	3.3	52
6	Size-dependent electroluminescence from Si quantum dots embedded in amorphous SiC matrix. Journal of Applied Physics, 2011, 110, .	2.5	45
7	Strong green-yellow electroluminescence from oxidized amorphous silicon nitride light-emitting devices. Applied Physics Letters, 2007, 90, 093515.	3.3	44
8	Role of barrier layers in electroluminescence from SiN-based multilayer light-emitting devices. Applied Physics Letters, 2008, 92, .	3.3	44
9	Structural and electronic properties of Si nanocrystals embedded in amorphous SiC matrix. Journal of Alloys and Compounds, 2011, 509, 3963-3966.	5.5	43
10	Oxygen induced strong green light emission from low-temperature grown amorphous silicon nitride films. Applied Physics Letters, 2006, 89, 221120.	3.3	40
11	Fabrication of large-scale periodic silicon nanopillar arrays for 2D nanomold using modified nanosphere lithography. Applied Surface Science, 2007, 253, 9035-9038.	6.1	40
12	Visible light emission from single layer Si nanodots fabricated by laser irradiation method. Applied Physics Letters, 2006, 89, 163107.	3.3	37
13	High-conductive nanocrystalline silicon with phosphorous and boron doping. Applied Surface Science, 2010, 257, 1337-1341.	6.1	37
14	Red–green–blue light emission from hydrogenated amorphous silicon carbide films prepared by using organic compound xylene as carbon source. Applied Physics Letters, 1998, 72, 13-15.	3.3	36
15	The influence of the growth conditions on the structural and optical properties of hydrogenated amorphous silicon carbide thin films. Journal of Alloys and Compounds, 1999, 290, 273-278.	5.5	36
16	Sensing mechanism of Sb, S doped SnO2 (1 1 0) surface for CO. Applied Surface Science, 2020, 502, 144	1406.1	34
17	Field emission from a periodic amorphous silicon pillar array fabricated by modified nanosphere lithography. Nanotechnology, 2008, 19, 135308.	2.6	33
18	New Self-Limiting Assembly Model for Si Quantum Rings on Si(100). Physical Review Letters, 2007, 98, 166102.	7.8	32

#	Article	IF	CITATIONS
19	Enhanced electroluminescence efficiency of oxidized amorphous silicon nitride light-emitting devices by modulating Siâ^•N ratio. Applied Physics Letters, 2007, 91, .	3.3	32
20	Light Trapping and Downâ€Shifting Effect of Periodically Nanopatterned Siâ€Quantumâ€Dotâ€Based Structures for Enhanced Photovoltaic Properties. Particle and Particle Systems Characterization, 2014, 31, 459-464.	2.3	32
21	Fabrication of Ordered SnO2 Nanostructures with Enhanced Humidity Sensing Performance. Sensors, 2017, 17, 2392.	3.8	32
22	Green electro- and photoluminescence from nanocrystalline Si film prepared by continuous wave Ar+ laser annealing of heavily phosphorus doped hydrogenated amorphous silicon film. Applied Physics Letters, 1998, 73, 105-107.	3.3	29
23	The dependence of the interface and shape on the constrained growth of nc-Si in a-SiNx/a-Si:H/a-SiNxstructures. Journal of Physics Condensed Matter, 2002, 14, 10083-10091.	1.8	28
24	Contribution of multiple emitting centers to luminescence from Si/SiO2 multilayers with step by step thermal annealing. Solid State Communications, 2004, 131, 701-705.	1.9	26
25	Humidity sensing properties of morphology-controlled ordered silicon nanopillar. Applied Surface Science, 2014, 317, 970-973.	6.1	26
26	Enhanced broadband spectral response and energy conversion efficiency for hetero-junction solar cells with graded-sized Si quantum dots/SiC multilayers. Journal of Materials Chemistry C, 2015, 3, 12061-12067.	5.5	24
27	Hydrogen-induced recovery of photoluminescence from annealed a‣i:Hâ^•a‣iO2 multilayers. Journal of Applied Physics, 2005, 98, 033532.	2.5	21
28	Vacuum electron emission with low turn-on electric field from hydrogenated amorphous carbon thin films. Applied Physics Letters, 2001, 79, 141-143.	3.3	20
29	Higher than 60% internal quantum efficiency of photoluminescence from amorphous silicon oxynitride thin films at wavelength of 470 nm. Applied Physics Letters, 2014, 105, .	3.3	20
30	Time-resolved and temperature-dependent photoluminescence study on phosphorus doped Si quantum dots/SiO_2 multilayers with ultra-small dot sizes. Optical Materials Express, 2016, 6, 3233.	3.0	20
31	Direct observation of resonant energy transfer between quantum dots of two different sizes in a single water droplet. Applied Physics Letters, 2006, 89, 033121.	3.3	18
32	UV and blue light emission from SiC nanoclusters in annealed amorphous SiC alloys. Journal of Non-Crystalline Solids, 2006, 352, 1398-1401.	3.1	17
33	Improved emission efficiency of electroluminescent device containing nc-Si/SiO_2 multilayers by using nano-patterned substrate. Optics Express, 2010, 18, 917.	3.4	17
34	Structural and electroluminescent properties of Si quantum dots/SiC multilayers. Applied Surface Science, 2013, 269, 37-40.	6.1	17
35	Size dependence of optical eigenmodes in photonic quantum dots prepared by conformal deposition method. Applied Physics Letters, 2007, 90, 174101.	3.3	16
36	Nanoscale quantification of charge injection and transportation process in Si-nanocrystal based sandwiched structure. Nanoscale, 2013, 5, 9971.	5.6	16

#	Article	IF	CITATIONS
37	The flexoelectric effect associated size dependent pyroelectricity in solid dielectrics. AIP Advances, 2015, 5, .	1.3	16
38	Luminescence and resonant energy transfer of two sizes of CdTe quantum dots embedded in gelatin films. Journal of Materials Science, 2007, 42, 9696-9699.	3.7	15
39	Dynamics of high quantum efficiency photoluminescence from N-Si-O bonding states in oxygenated amorphous silicon nitride films. Applied Physics Letters, 2016, 108, .	3.3	15
40	Depth-dependent humidity sensing properties of silicon nanopillar array. Sensors and Actuators B: Chemical, 2016, 237, 526-533.	7.8	15
41	High-Performance Tapered Fiber Surface Plasmon Resonance Sensor Based on the Graphene/Ag/TiO2 Layer. Plasmonics, 2021, 16, 2291-2303.	3.4	15
42	Subband Light Emission from Phosphorous-Doped Amorphous Si/SiO 2 Multilayers at Room Temperature. Chinese Physics Letters, 2011, 28, 067802.	3.3	14
43	Surface potential modeling and reconstruction in Kelvin probe force microscopy. Nanotechnology, 2017, 28, 365705.	2.6	14
44	Formation of a dense nanocrystalline Si array on an insulating layer by laser irradiation of ultrathin amorphous Si films. Scripta Materialia, 2005, 53, 811-815.	5.2	13
45	Enhancement of electroluminescence from embedded Si quantum dots/SiO2multilayers film by localized-surface-plasmon and surface roughening. Scientific Reports, 2015, 5, 11881.	3.3	13
46	Enhanced photoluminescence from CdS with SiO2 nanopillar arrays. Scientific Reports, 2015, 5, 11375.	3.3	12
47	Properties of S-Functionalized Nitrogen-Based MXene (Ti2NS2) as a Hosting Material for Lithium-Sulfur Batteries. Nanomaterials, 2021, 11, 2478.	4.1	12
48	Enhanced green to red photoluminescence in thermally annealed of amorphous-Si:H/SiO2 multilayers. Thin Solid Films, 2006, 515, 2322-2325.	1.8	11
49	Luminescence behavior from amorphous silicon-carbide film-based optical microcavities. Materials Chemistry and Physics, 2008, 111, 279-282.	4.0	11
50	Field dependent electroluminescence from amorphous Si/SiNx multilayer structure. Applied Physics Letters, 2009, 94, 161101.	3.3	11
51	The role of N-Si-O bonding configurations in tunable photoluminescence of oxygenated amorphous silicon nitride films. Applied Physics Letters, 2015, 106, .	3.3	11
52	Characterization of Pt- or Pd-doped graphene based on density functional theory for H ₂ gas sensor. Materials Research Express, 2019, 6, 095603.	1.6	11
53	Sensitivity enhancement of WS ₂ -coated SPR-based optical fiber biosensor for detecting glucose concentration*. Chinese Physics B, 2020, 29, 110701.	1.4	11
54	Fabrication of highly ordered metallic arrays and silicon pillars with controllable size using nanosphere lithography. Physica E: Low-Dimensional Systems and Nanostructures, 2009, 41, 1600-1603.	2.7	10

#	Article	IF	CITATIONS
55	Microscopic and macroscopic characterization of the charging effects in SiC/Si nanocrystals/SiC sandwiched structures. Nanotechnology, 2014, 25, 055703.	2.6	10
56	Improved power efficiency in phosphorus doped n-a-SiNxOy/p-Si heterojunction light emitting diode. Applied Physics Letters, 2017, 110, 081109.	3.3	10
57	Surface potential extraction from electrostatic and Kelvin-probe force microscopy images. Journal of Applied Physics, 2018, 123, .	2.5	10
58	Morphology control and electron field emission properties of high-ordered Si nanoarrays fabricated by modified nanosphere lithography. Applied Surface Science, 2009, 255, 5414-5417.	6.1	9
59	On-chip silicon-based active photonic molecules by complete photonic bandgap light confinement. Applied Physics Letters, 2011, 99, 034105.	3.3	9
60	Strong blue light emission from a-SiNx:O films via localized surface plasmon enhancement. Applied Physics Letters, 2012, 101, .	3.3	9
61	Comparative study of electroluminescence from annealed amorphous SiC single layer and amorphous Si/SiC multilayers. Journal of Non-Crystalline Solids, 2012, 358, 2114-2117.	3.1	9
62	Fabrication and characteristics of N-I-P structure amorphous silicon solar cells with CdS quantum dots on nanopillar array. Physica E: Low-Dimensional Systems and Nanostructures, 2019, 109, 152-155.	2.7	9
63	Charge transfer of single laser crystallized intrinsic and phosphorus-doped Si-nanocrystals visualized by Kelvin probe force microscopy. Journal of Applied Physics, 2014, 116, 134309.	2.5	8
64	Organic Vapour Sensing Properties of Area-Ordered and Size-Controlled Silicon Nanopillar. Sensors, 2016, 16, 1880.	3.8	8
65	Simulation and Experimental Study on Anti-reflection Characteristics of Nano-patterned Si Structures for Si Quantum Dot-Based Light-Emitting Devices. Nanoscale Research Letters, 2016, 11, 317.	5.7	8
66	Novel photoluminescence from hydrogenated amorphous carbon films prepared by using xylene source. Journal of Materials Research, 2001, 16, 325-328.	2.6	7
67	Room temperature electron tunneling and storage in a nanocrystalline silicon floating gate structure. Journal of Non-Crystalline Solids, 2004, 338-340, 318-321.	3.1	7
68	Capacitance characteristics of metal-oxide-semiconductor capacitors with a single layer of embedded nickel nanoparticles for the application of nonvolatile memory. Chinese Physics B, 2010, 19, 047308.	1.4	7
69	Enhanced Humidity Sensitivity with Silicon Nanopillar Array by UV Light. Sensors, 2018, 18, 660.	3.8	7
70	Effects of hydrogen plasma annealing on the luminescence from a-Si:H/SiO2 and nc-Si/SiO2 multilayers. Applied Surface Science, 2007, 253, 8647-8651.	6.1	6
71	Annealing effect on structures and luminescence of amorphous SiN films. Materials Letters, 2007, 61, 5010-5013.	2.6	6
72	Enhanced luminescence from Si quantum dots/SiO2 multilayers by hydrogen annealing. Journal of Non-Crystalline Solids, 2012, 358, 2141-2144.	3.1	6

#	Article	IF	CITATIONS
73	The role of N _{<i>x</i>} –Si–O _{<i>y</i>} bonding configuration in acquiring strong blue to red photoluminescence from amorphous SiN _{<i>x</i>} O _{<i>y</i>} film. Canadian Journal of Physics, 2014, 92, 602-605.	1.1	6
74	Observation of "fast―and "slow―decay processes in oxygen-doped hydrogenated amorphous silicon nitride thin films. Optical Materials Express, 2015, 5, 22.	3.0	6
75	Sensing mechanism of hydrogen storage on Li, Na and K-decorated Ti2C. Applied Physics A: Materials Science and Processing, 2020, 126, 1.	2.3	6
76	Promoting sensitivity and selectivity of NO2 gas sensor based on (P,N)-doped single-layer WSe2: A first principles study. Results in Physics, 2022, 34, 105296.	4.1	6
77	The Role of N–Si–O Defect States in Optical Gain from an aâ€SiN <i>_x</i> O <i>_y</i> /i>/SiO ₂ Waveguide and in Light Emission from an nâ€aâ€SiN _x O _y /pâ€Si Heterojunction LED. Physica Status Solidi (A) Applications and Materials Science. 2018. 215. 1700750.	1.8	5
78	Calculating electrostatic interactions in atomic force microscopy with semiconductor samples. AIP Advances, 2019, 9, .	1.3	5
79	Innovative all-silicon based a-SiNx:O/c-Si heterostructure solar-blind photodetector with both high responsivity and fast response speed. APL Photonics, 2022, 7, .	5.7	5
80	Conformal coverage for two-dimensional arrays of microcavites with quasi-three dimensional confinement by distributed Bragg reflectors. Applied Surface Science, 2007, 253, 4254-4259.	6.1	4
81	Charge storage and light emission properties of three dimension controllable Si nanostructures. Physica Status Solidi C: Current Topics in Solid State Physics, 2009, 6, 721-727.	0.8	4
82	First principle study on gas sensor mechanism of black-AsP monolayer. Wuli Xuebao/Acta Physica Sinica, 2021, 70, 157101.	0.5	4
83	A separable nonlinear least squares approach for double-diode photovoltaic model parameter extraction. Journal of Renewable and Sustainable Energy, 2021, 13, .	2.0	4
84	Nanoscale Characterization of Active Doping Concentration in Boronâ€Doped Individual Si Nanocrystals. Physica Status Solidi (A) Applications and Materials Science, 2018, 215, 1800531.	1.8	3
85	The role of potassium in grain boundaries of flexible CZTSSe thin film solar cells. Journal of Materials Science: Materials in Electronics, 2018, 29, 17503-17507.	2.2	3
86	Enhanced Humidity Sensing Response of SnO2/Silicon Nanopillar Array by UV Irradiation. Sensors, 2019, 19, 2141.	3.8	3
87	Charging and Coulomb blockade effects of the nc-Si embedded in SiNx double-barrier structures. Journal of Non-Crystalline Solids, 2006, 352, 1126-1129.	3.1	2
88	Pyroelectric property of SrTiO ₃ /Si ferroelectric-semiconductor heterojunctions near room temperature. Journal of Advanced Dielectrics, 2015, 05, 1550031.	2.4	2
89	Controlled Fabrication of Si Nanowires with Nanodots Using Nanosphere Lithography. Journal of Nanoscience and Nanotechnology, 2016, 16, 1537-1540.	0.9	2
90	Physical properties in polydomain c/a/c/a phase PbTiO3 ferroelectric thick films: effect of thermal stresses. Applied Physics A: Materials Science and Processing, 2017, 123, 1.	2.3	2

#	Article	IF	CITATIONS
91	Sub-100 nm Single Crystalline Periodic Nano Silicon Wire Obtained by Modified Nanoimprint Lithography. Nanoscience and Nanotechnology Letters, 2013, 5, 737-740.	0.4	2
92	Fabrication and characterization of Si nanotip arrays for Si-based nano-devices. , 2008, , .		1
93	Optical absorption and charging effect in nano-crystalline Ge/SiNx multilayers. Applied Surface Science, 2013, 269, 129-133.	6.1	1
94	Microscopic and Macroscopic Bipolar Injection and Carrier Recombination in Single-layer Si Nanocrystals. IOP Conference Series: Materials Science and Engineering, 2018, 436, 012003.	0.6	1
95	Inhomogeneous probe surface induced effect in Kelvin probe force microscopy. Journal of Applied Physics, 2020, 127, 184302.	2.5	1
96	Design and Research of Enhanced LED Performance Based on Graphical Substrate with Multilayer Hyperbolic Metamaterials. Plasmonics, 2021, 16, 1593-1604.	3.4	1
97	RESONANT TUNNELING AND COULOMB BLOCKADE IN A NANOCRYSTALLINE SI DOUBLE-BARRIER FLOATING-GATE STRUCTURE. International Journal of Nanoscience, 2006, 05, 853-858.	0.7	0
98	Photonic quantum dots based on Bragg reflectors grown by conformal deposition on patterned substrates. Applied Surface Science, 2008, 254, 4211-4215.	6.1	0
99	The evolution of photoluminescence in oxidized amorphous silicon nitride films by rapid thermal annealing. Journal Physics D: Applied Physics, 2008, 41, 165411.	2.8	0
100	Silicon based photonic quantum dots. , 2008, , .		0
101	Intense green light emission from low temperature grown SiNO complex system. , 2008, , .		0
102	Filed emission characterizes of size-controllable Si nanopillar arrays. EPJ Applied Physics, 2010, 51, 20601.	0.7	0
103	Low turn-on and high efficient oxidized amorphous silicon nitride light-emitting devices induced by high density amorphous silicon nanoparticles. Thin Solid Films, 2010, 518, 3938-3941.	1.8	0
104	Si-based photonic quantum dots with the self-similar distributed Bragg reflectors. Thin Solid Films, 2011, 519, 3295-3300.	1.8	0
105	Two-Dimensional Cavity Resonant Modes of Si Based Bragg Reflection Ridge Waveguide. Chinese Physics Letters, 2011, 28, 066803.	3.3	0
106	Charging effect in silicon nanocrystals observed by electrostatic and Kelvin-probe force microscopy. , 2014, , .		0
107	Charge storage in Si-nanocrystals embedded NOS structure characterized by Kelvin probe force microscopy. , 2016, , .		0
108	Design of a Microwave Power Detection System in the 5G-Communication Frequency Band. Sensors, 2021, 21, 2674.	3.8	0

#	Article	IF	CITATIONS
109	Effect of Prefabricated Layer Structure on Properties of CZTS Thin Films and Solar Cells. IOP Conference Series: Earth and Environmental Science, 2020, 571, 012033.	0.3	Ο